

HI 21cm absorption in two low redshift damped Ly α systems

W. Lane, A. Smette¹, F. Briggs

Kapteyn Astronomical Institute, P.O. Box 800, NL-9700 AV Groningen, The Netherlands

S. Rao, D. Turnshek

Dept. of Physics and Astron., Univ. of Pittsburgh, Pittsburgh, PA 15260, USA

and

G. Meylan

ESO, Karl-Schwarzschild-Strasse 2, D-85748 Garching bei München, Germany

ABSTRACT

We report the discovery of two low redshift HI 21cm absorbers, one at $z = 0.2212$ towards the $z_{em} = 0.630$ quasar OI 363 (B0738+313), and the other at $z = 0.3127$ towards PKS B1127-145 ($z_{em} = 1.187$). Both were found during a survey of MgII selected systems at redshifts $0.2 < z < 1$ using the new UHF-high system at the Westerbork Synthesis Radio Telescope (WSRT). New HST/FOS observations also identify both systems as damped Ly α (DL α) absorbers. By comparing the column density from the DL α line with that from the HI 21cm line, we calculate the spin temperature, T_s of the two systems. We find $T_s \approx 1000$ K for both of these low redshift absorbers.

For the $z = 0.3127$ system towards PKS B1127-145, two galaxies have been previously identified with emission lines at the absorber redshift (Bergeron & Boissé, 1991), with the galaxy at a closer projected distance to the quasar assumed to be responsible for the absorption system. An ESO-NTT/EFOSC2 spectrum of a 3rd, fainter companion at 3.9 arcsec or $11 h_{100}^{-1} kpc$ from the line of sight of PKS 1127-145 reveals [OIII]4958 and 5007 at $z = 0.3121 \pm 0.0003$. We consider this object the most likely to be responsible for the 21cm absorption, as it is much closer to the QSO sightline than the two galaxies identified by Bergeron & Boissé.

Subject headings: quasars: absorption lines — quasars: individual(PKS B1127-145, OI 363) — galaxies:ISM

1. Introduction

The study of low redshift examples of the quasar absorption line systems responsible for the damped Ly α (DL α) and HI 21cm absorption lines is important to help bridge our understanding of neutral gas-rich systems between those at redshift $z = 0$ and those at high z . Our knowledge of the neutral gas in nearby spiral galaxies is mainly based on observations of the HI 21cm line in emission. At high redshift, however, we observe the HI 21cm line in absorption, which can only be seen along a limited number of lines of sight through the intervening absorber, making detailed knowledge of the gas characteristics difficult. The low redshift ($z < 1$) neutral absorbers are still close enough that both optical and radio data of reasonable

¹current address: NASA/GSFC, Code 681, Greenbelt, MD 20771, USA

quality can be obtained in order to understand their kinematics and physical gas characteristics. Such information is necessary to build a framework for a correct interpretation of the higher z counterparts to these systems.

Searches for redshifted HI 21cm absorption can be time-consuming since radio spectrometers typically observe only relatively narrow instantaneous bandwidths and only the highest column density QSO absorption line systems have measurable optical depths in the 21cm line. Since DLa systems have high column densities of neutral HI, they are the most likely objects to have HI 21cm absorption. Unfortunately for low redshift work, the Ly α line is not shifted into the optical window until $z \simeq 1.65$, so finding these lines requires UV spectra to be taken with space telescopes. This, combined with the small cross section for DLa absorption, means that only a small number of DLa systems have been identified at low redshift. Therefore, alternative selection criteria which are reasonably effective at finding an HI 21cm absorber must be used.

All known DLa and HI 21cm absorbers have associated low-ionization metal lines (cf. Lu and Wolfe, 1994) such as the MgII $\lambda\lambda 2796, 2803$ doublet, which can be observed easily in ground-based spectra down to about $z = 0.1$. A study of MgII selected systems using previously existing UV data yielded about 1 DLa system per 10 MgII systems observed (Rao, et al., 1995). A similar statistic exists for HI 21cm absorption in MgII systems (Briggs & Wolfe, 1983). This suggests that MgII can be used to optically select systems likely to have high column densities of neutral gas observed either as DLa or HI 21cm absorption.

We are conducting a survey for HI 21cm absorption in low redshift MgII selected systems using the Westerbork Synthesis Radio Telescope (WSRT). In this paper we present two new HI 21cm absorbers from our survey, one towards PKS B1127-145 at $z = 0.3127$ and the other towards OI 363 at $z = 0.2212$. Recent HST/FOS spectra have identified DLa absorption in both of these objects as well.

2. Radio Observations

PKS 1127-145 was observed for 60 minutes on 16 March 1997, and OI 363 for 90 minutes on 27 April 1997 using the new UHF-high system (700-1200 MHz) at the WSRT. Observation length was determined by the amount of time needed to reduce the noise level in the spectra to 1% or less of the background quasar flux level. A bandwidth of 2.5 MHz was centered at the expected absorption frequency based on the MgII absorption redshift of each system. This was divided into 128 channels at spacings of 5 km s^{-1} for OI 363 and 5.4 km s^{-1} for PKS B1127-145. We used a uniform spectral taper, so the effective velocity resolution is 1.2 times the channel spacing, or 6 and 6.5 km s^{-1} for the respective absorption systems. Due to limitations in the DXB spectrometer and the ongoing upgrade at the WSRT, not all of the interferometers in the array were available. The OI 363 observation had 24 interferometers in each of two orthogonal linear polarizations. For PKS B1127-145, 28 interferometers in one polarization and 21 in the other were used.

Both data sets were processed identically. Standard programs in the NEWSTAR data reduction package were used for initial data calibration and editing. The bandpass was calibrated by observations of 3C286 made before and after each object observation. The data were then moved to AIPS for further processing. Using the routine CALIB, the data were self-calibrated in phase to a point source model of the field to correct for residual phase errors. Side-lobe interference from other strong sources in the field away from the phase center was not a problem in either data set. The continuum flux was subtracted from the visibility data using the algorithm UVLIN, which finds a linear fit to the complex spectrum measured at each u-v point, and then subtracts the fit from the spectrum (Cornwell, et al., 1992).

Spectral line image cubes were synthesized from the continuum subtracted data using the task IMAGR. The data were given a natural weighting to reduce the noise as much as possible. The slight loss of angular resolution in the WSRT synthesized beam resulting from this weighting does not affect our spectra, because PKS B1127-145 and OI 363 are both compact sources, much smaller than the beam of the WSRT at these frequencies. The image cubes were hanning smoothed in frequency but not resampled. The final spectra are shown in figs. 1 and 2. Absorption line characteristics derived from fitted gaussians are summarized in Table 1.

3. HST Spectroscopy

UV spectra of OI 363 and PKS1127–145 were obtained with the *HST* Faint Object Spectrograph through the G160L/BL grating-digicon combination. These QSOs were part of a large survey designed to identify the nature of the Ly α line in known MgII absorption-line systems. The survey spectra and results will be presented elsewhere (Rao & Turnshek, 1998).

The spectra of OI 363 and PKS1127–145 revealed DLa absorption lines at the redshift of the intervening MgII absorption systems. The column density that best fit the data was determined by minimizing the least squares difference between the data and the fit within the core of the damped line. The largest uncertainty in the column density comes from continuum placement. Therefore, a conservative estimate of the uncertainty was determined by placing new continua at levels corresponding to 1σ above and below the original continuum, re-normalising the spectrum, and re-determining the best fit to the damping profile in each case. The column density of the OI 363 absorption-line system was measured to be $7.9 \pm 1.4 \times 10^{20} \text{ cm}^{-2}$, while that of the PKS1127–145 system was measured to be $5.1 \pm 0.9 \times 10^{21} \text{ cm}^{-2}$.

4. Optical Data

Optical observations of PKS B1127-145 and objects in the surrounding field were made on 21 May 1990 with the EFOSC 2 instrument installed at one of the Nasmyth foci of the ESO-3.5m NTT telescope, at La Silla, Chile. The detector used was the 1024 x 1024 pixels Thomson CCD # 17, providing a pixel scale of 0.153 arcsec/pixel. The observing run was originally aimed at finding secondary images of highly-luminous quasars due to gravitational lensing (cf. Surdej, et al., 1989). R- and B-Band images with 5 minute exposures indicated the presence of two faint companions to the QSO, with B-R colors compatible with those expected for lensed secondary images. No standard stars were observed in these filters.

In order to check if one or both companions were indeed a secondary lensed image, two 30-minute spectra were obtained with grism # 6 and a 1.472''-wide slit oriented to include both objects and the QSO (P.A. = 8.4deg). The spectra were wavelength calibrated with He and Ar arc lamp exposures taken immediately after the observation. The wide slit, chosen to include as much light as possible from the companion objects, leads to a poor resolution of only 27 Å(FWHM).

The spectra of both companions indicate that they are galaxies, and not additional, lensed images of the quasar. Thus there is no evidence for lensing in this system. The companion object to the east shows no emission lines, and the S/N in the continuum is not good enough to determine its redshift. However, the companion to the west does show [OIII]4958 and [OII]5007 emission at $z = 0.3121 \pm 0.0003$, making it a candidate object for causing the neutral hydrogen absorption at similar redshift. The emission spectrum is

shown in fig. 3.

5. Spin Temperature

If a system is both a DLa absorber and an HI 21cm absorber, a comparison of the neutral HI column density derived from the two different absorption lines allows a determination of the mean spin temperature, T_s , of the absorbing gas. The equation relating neutral hydrogen column density, $N(\text{HI})$, to the observed HI 21cm absorption profile is:

$$N(\text{HI}) = 1.8 \times 10^{18} \frac{T_s}{f} EW_{21} \text{ cm}^{-2}$$

where f is the fraction of the continuum source covered by the absorber, T_s is the spin temperature of the gas, and EW_{21} is the integral of the optical depth over velocity. For a single line with a Gaussian profile, $\tau(v)$,

$$EW_{21} = 1.06 \times \tau_c \Delta V$$

where τ_c is the peak optical depth of the line at the line center and ΔV is the FWHM velocity in km s^{-1} .

Since both of the background radio quasars in this study are quite compact, we assume that the covering factor, $f = 1$. We also assume the same gas is responsible for the 21cm absorption and the DLa, and use the $N(\text{HI})$ from the DLa line, to calculate the spin temperature of the gas. We find $T_s = 1230 \pm 335$ K for OI 363, and $T_s = 1000 \pm 200$ K for PKS B1127-145.

When calculated in this way, the spin temperature represents a column density weighted harmonic mean temperature of all the gas along the line of sight. Since the gas is most likely composed of more than one temperature phase, the spin temperature value does not have a straightforward interpretation (cf. Carilli, et al. 1996). However, in the simplest sense, it can be understood as an upper limit to the temperature of the gas in the coldest phase.

6. Discussion

6.1. OI 363

OI 363 (0738+313), is a core dominated quasar at $z_{em} = 0.630$. Observations at 1640 MHz (Murphy, et al., 1993) show that the lobes extending $\approx 30''$ from the core contain only 3% of the total flux of the quasar. The quasar is slightly variable at low frequencies (Bondi, et al., 1996b).

The metal line absorption system was originally reported by Boulade, et al. (1987) at a redshift of $z = 0.2213$, and subsequently by Boissé, et al. (1992) at a redshift of $z = 0.2216 \pm 0.0003$. The only identified lines in the spectrum are the MgII $\lambda\lambda 2796, 2803$ doublet and a possible MgI line. Deep optical imaging was made by LeBrun et al. (1993), who identified what they considered a likely absorber at a projected separation from the quasar of $5.70''$, or $1.24R_H$ if it lies at $z = 0.221$. They identified three additional galaxies, at smaller angular separations from the quasar, which are very faint and would be dwarf galaxies at the absorption redshift. Unfortunately, they do not report a confirmed redshift for any object in the field near the quasar.

The HI 21cm absorption line, shown in fig. 1, has a narrow width of only two channels over most of its depth, and may be unresolved by this observation. This implies an upper limit to the line width

of $\sim 8 \text{ km s}^{-1}$ at the 6 km s^{-1} resolution of the data. The HI column density from the DLa profile is $N(\text{HI}) = 7.9 \pm 1.4 \times 10^{20} \text{ cm}^{-2}$, and the calculated mean harmonic spin temperature is $T_s = 1230 \pm 335 \text{ K}$. The thermal kinetic temperature of the gas for a line of width 8 km s^{-1} is $T_k = 1400 \text{ K}$. This means that within the errors, $T_s = T_k$.

6.2. PKS B1127-145

PKS B1127-145 is a compact, gigahertz peaked radio source at $z = 1.187$. VLBI observations at 1670 MHz show a slightly elongated structure with an extent of approximately 20 mas. Observations at 408 MHz give a flux variability of 1.2 Jy/year (Bondi, et al., 1996a), and indicate structural variations as well.

Fig. 2 shows the neutral HI 21cm absorption for this system. The observed flux of the quasar is 5.25 Jy in this observation. This is somewhat lower than reported fluxes in NED², however, as discussed above the quasar is a known variable at low frequency. If the absorption line is fit by one gaussian component, the optical depth of the absorption is 6.2%, and the FWHM is approximately 42 km s^{-1} . However, there is some evidence for structure in the line. In particular, the split in the middle appears to be real, suggesting at least two components, and the asymmetric low frequency side of the profile may result from a third component. There is some low level interference in the spectrum adjacent to the low frequency side of the absorption line, at $\sim 1081.75 \text{ MHz}$, which makes interpretation of the real shape difficult. The HI column density from the DLa profile is $N(\text{HI}) = 5.1 \pm 0.9 \times 10^{21} \text{ cm}^{-2}$, and the calculated $T_s = 1000 \pm 200 \text{ K}$.

Bergeron and Boissé (1991) studied this $z_{abs} = 0.313$ metal-line system in some detail. They identify MgII, FeII and MgI absorption in the spectrum. The average redshift of the metal lines is $z = 0.3127 \pm 0.0002$. In addition to the absorption spectrum, and deep images of the field, they present emission spectra for two of the bigger bright galaxies near the quasar (different from the two faint companions discussed in Sect. 4), both of which have redshifts similar to that of the metal line system. They identify the galaxy at the smaller projected distance from the quasar sightline as the absorber.

The ESO/EFOSC2 spectral observations (discussed in Sect. 3) identify a new candidate absorber galaxy for this system. The new emission object is a close companion to the west of the quasar and lies at a projected distance of $3.9''$ or $11 h_{100}^{-1} \text{ kpc}$ from the quasar sightline. Based on comparison with other objects in our image for which apparent magnitudes are given in Bergeron and Boissé (1991), it has an apparent magnitude of $m_r = 22.3$. The galaxy which Bergeron and Boissé identify as the absorber is at a projected separation of $9.6''$, or $37 h_{100}^{-1} \text{ kpc}$ from the quasar at the redshift of the galaxy. This corresponds to a galactic radius of $2.7 R_H$. A column density of neutral gas of 10^{21} cm^{-2} is unlikely at this galactic radius, and we consider the new emission object, although smaller and fainter, to be the more likely absorber given its proximity to the quasar sightline. It is also possible that the three galaxies at similar redshift have undergone strong interaction with each other, in which case the absorbing gas could be tidal debris.

²The NASA/IPAC Extragalactic Database (NED) is operated by the Jet Propulsion Laboratory, California Institute of Technology, under contract with the National Aeronautics and Space Administration.

6.3. Spin Temperature

Fig. 4 shows T_s vs. redshift for all of the known HI 21cm and DLa absorber systems, calculated from the literature (as summarized by Carilli, et al., 1996), with the two new data points marked by open symbols. The shaded region shows the range of Galactic T_s values at optical depths comparable to those found in the DLa systems, using numbers from Braun and Walterbos (1992). The large errorbars in any given measurement are dominated by uncertainties in the true optical continuum level, due to confusion from the Ly α forest lines, which make fitting the damped profile difficult. As noted in previous studies (cf. de Bruyn, et al. 1996), all of the redshifted absorbers except the highest optical depth (lowest T_s) system have T_s values which are roughly two or more times greater than the Galactic values at similar optical depths.

Most estimates of T_s for the present epoch have been based on studies of the Milky Way or Andromeda (cf. Dickey and Brinks (1988); Braun and Walterbos (1992), and references therein). These estimates use column densities derived from HI 21cm emission lines rather than from DLa absorption lines, but studies have shown that $N(\text{HI})_{\text{Ly}\alpha} \approx N(\text{HI})_{21\text{cm}}$ (Dickey and Lockman, 1990). This suggests that T_s values for the galaxy and the redshifted DLa systems, although calculated from different quantities, can be compared.

On the other hand, values for T_s have a strong correlation with the column density, $N(\text{HI})$, in each of the clouds along the line of sight in the Galaxy, and are thus sensitive to the location of individual gas clouds. A single cloud usually has a greater angular size on the sky than the beam with which it is observed, so it is possible to calculate the spin temperature for just one cloud. This is not the case in redshifted systems, where a line of sight includes more of the galaxy and possibly many clouds. Thus it is difficult to usefully compare present epoch spin temperature values to those calculated at higher redshifts.

The new systems in this study were observed at low redshift with the same line of sight limitations as the higher redshift systems, allowing a meaningful comparison. There is no clear trend for a change in T_s with increasing redshift among the eight systems shown in Fig. 4. If the gap between T_s values in the galaxy and those in the DLa systems is an effect of evolution over time, then all of that evolution must have occurred between $z = 0.2$ and the present epoch. Instead, we consider it more likely that the gap arises from the presence of many clouds in one line of sight at high redshift, or from differences in the radio and optical sightlines.

The sizes of the radio emission regions of quasars are much larger than the optical regions, and usually larger than an average cloud as well. It is therefore likely that the optical and radio lines of sight actually sense different clouds in a redshifted galaxy, and hence have different column densities of neutral gas. This implies that the spin temperatures derived by assuming both column densities are equal may be meaningless. Unfortunately, the resolution obtained in most radio survey observations (with single dishes or synthesized beams from arrays like the WSRT) is at least as large on the sky as compact background radio sources, and gives no spatial information about the clouds in front of the quasar. Future use of VLBI techniques to pinpoint the radio sightlines more accurately may help to clarify this problem.

This research has made use of the NASA/IPAC Extragalactic Database (NED) which is operated by the Jet Propulsion Laboratory, California Institute of Technology, under contract with the National Aeronautics and Space Administration.

REFERENCES

- Bergeron, J. & Boissé, P, 1991, A&A 243, 344
- Boissé, P., Boulade, O., Kunth, D., Tytler, D., & Vigroux, L., 1992, A&A, 262, 401
- Bondi, M., Padrielli, L., Fanti, R., Ficarra, A., Gregorini, L., Mantovani, F., Bartel, N., Romney, J.D., Nicolson, G.D., & Weiler, K.W., 1996a, A&A, 308, 415
- Bondi, M., Padrielli, L., Fanti, R., Ficarra, A., Gregorini, L., & Mantovani, F., 1996b, A&AS, 120, 89
- Boulade, O., Kunth, D., Tytler, D., & Vigroux, L., 1987, in High Redshift and Primeval Galaxies, edited by J. Bergeron *et al.* (France: Edit. Front.), p. 349
- Braun, R., & Walterbos, R., 1992, ApJ, 386, 120
- Briggs, F. & Wolfe, A., 1983, 268, 76
- de Bruyn, A.G., O’Dea, C.P., & Baum, S.A., 1996, A&A, 305, 450
- Carilli, C.L., Lane, W., de Bruyn, A.G., Braun, R., & Miley, G.K., 1996, AJ 111 1830
- Cornwell, T.J., Uson, J.M., & Haddad, N., 1992, A&A, 258, 583
- Dickey, J.M., & Brinks, E. 1988, MNRAS, 233, 781
- Dickey, J.M., & Lockman, F.J. 1990, ARA&A, 28, 215
- Le Brun, V., Bergeron, J., Boisse, P., & Christian, C., 1993, A&A, 279, 33
- Lu, L., & Wolfe, A.M., 1994, AJ, 108, 44
- Murphy, D.W., Browne, I.W.A., & Perley, R.A., 1993, MNRAS, 264, 298
- Rao, S.M., Turnshek, D.A., & Briggs, F.H., 1995, ApJ, 449, 488
- Rao, S.M., Turnshek, D.A., 1998, in prep.
- Surdej, J., Arnaud, J., Borgeest, U., Djorgovski, S., Fleischmann, F., Hammer, F., Hutsemekers, D., Kayser, R., Lefevre, O., Nottale, L., Magain, P., Meylan, G., Refsdal, S., Remy, M., Shaver, P., Smette, A., Swings, J.P., Vanderriest, C., Van Drom, E., Veron Cetty, M., Veron, P., & Weigelt, G., 1989, The Messenger, 55, 8

Fig. 1.— Spectrum from a 90 minute WSRT observation of OI 363 showing HI 21cm absorption at $z = 0.2212$. The rms noise is 14 mJy/channel, and the velocity spacing is 5 km s^{-1} . Data have been given a natural weight and hanning smoothed but not resampled. The expected frequency for absorption is based on a low resolution redshift for MgII absorption in this system (Boisse, et al. 1992). The MgII absorption is much broader in velocity and comes from gas of lower HI column density, which accounts for its slight redshift offset from the HI 21cm line.

Fig. 2.— Spectrum from a 60 minute WSRT observation of PKS B1127-145 showing HI 21cm absorption at $z = 0.3127$. The rms noise is 14 mJy/channel, and the velocity spacing is 5.4 km s^{-1} . Data have been given a natural weight and hanning smoothed, but not resampled. The frequency at which absorption was expected based on the metal absorption lines (Bergeron and Boissé, 1991) is marked and the standard deviation of this value is shown.

Fig. 3.— ESO/EFOSC2 emission spectrum for small companion galaxy close to the line of sight PKS B1127-145, showing [OIII]4958 and [OII]5007 emission at $z = 0.3121 \pm 0.0003$.

Fig. 4.— Plot of T_s vs. redshift, for all known high redshift HI 21cm/damped Ly α absorbers. Open points from this study. Filled squares calculated from the literature, as summarized by Carilli et al. (1996). Values of optical depth for the absorbers fall in the range $0.02 < \tau < 0.7$. The shaded region shows the range of T_s values in the Milky Way for optical depths in the range $0.01 < \tau < 1$ (Braun and Walterbos, 1992). T_s is generally larger for smaller optical depth systems.

Table 1: Absorption information

	PKS B1127-145	OI 363
z_{em}	1.187	0.630
z_{abs}	0.3127 ± 0.0002	0.2212 ± 0.0001
21cm line depth (mJy)	330 ± 14	82 ± 14
S_ν continuum (mJy)	5285 ± 11	1940 ± 5
21cm optical depth, τ_c	0.062 ± 0.003	0.042 ± 0.007
21cm FWHM (km s^{-1})	42.1 ± 2.7	8 ± 1
$N(\text{HI})_{DL\alpha}$ (cm^{-2})	$5.1 \pm 0.9 \times 10^{21}$	$7.9 \pm 1.4 \times 10^{20}$
T_s (K)	1000 ± 200	1230 ± 335

Figure 1

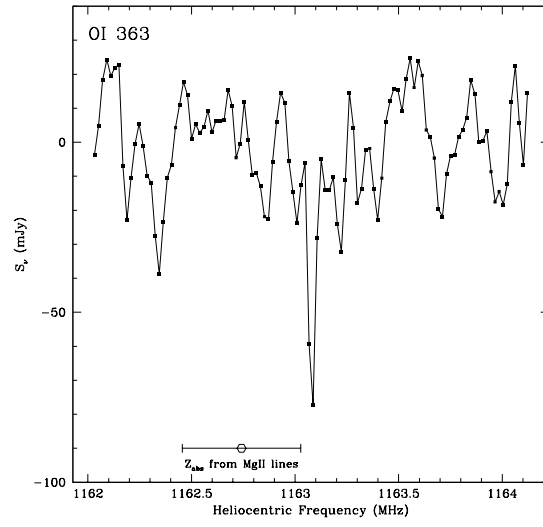


Figure 2

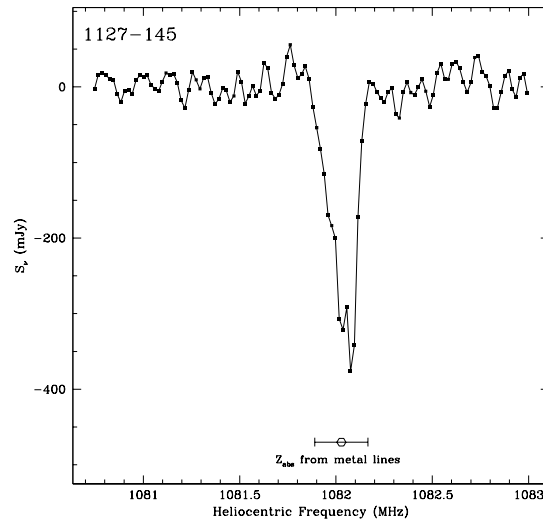


Figure 3

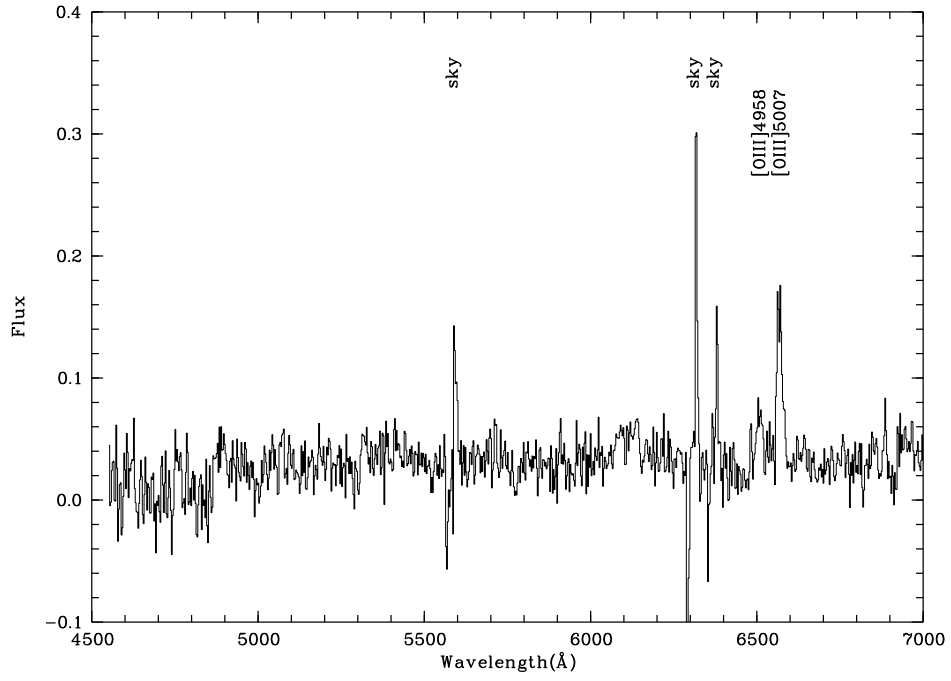


Figure 4

